Digestive Diseases and Sciences (2019) 64:2854–2866
https://doi.org/10.1007/s10620-019-05622-6

ORIGINAL ARTICLE

The Proton Pump Inhibitor Lansoprazole Has Hepatoprotective Effects in In Vitro and In Vivo Rat Models of Acute Liver Injury

Richi Nakatake[1] · Hidehiko Hishikawa[1] · Masaya Kotsuka[1] · Morihiko Ishizaki[1] · Kosuke Matsui[1] · Mikio Nishizawa[2] · Katsuhiko Yoshizawa[3] · Masaki Kaibori[1] · Tadayoshi Okumura[1,4]

Received: 29 December 2018 / Accepted: 8 April 2019 / Published online: 15 April 2019

Abstract

Background/Aims The proton pump inhibitor lansoprazole (LPZ) is clinically used to reduce gastric acid secretion, but little is known about its possible hepatoprotective effects. This study aimed to investigate the hepatoprotective effects of LPZ and its potential mechanisms using in vitro and in vivo rat models of liver injury.

Methods For the in vitro model of liver injury, primary cultured rat hepatocytes were treated with interleukin-1β in the presence or absence of LPZ. The influence of LPZ on inducible nitric oxide synthase (iNOS) induction and nitric oxide (NO) production and on the associated signaling pathways was analyzed. For the in vivo model, rats were treated with D-galactosamine (GalN) and lipopolysaccharide (LPS). The effects of LPZ on survival and proinflammatory mediator expression (including iNOS and tumor necrosis factor-α) in these rats were examined.

Results LPZ inhibited iNOS induction partially through suppression of the nuclear factor-kappa B signaling pathway in hepatocytes, thereby reducing potential liver injury from excessive NO levels. Additionally, LPZ increased survival by 50% and decreased iNOS, tumor necrosis factor-α, and cytokine-induced neutrophil chemoattractant-1 mRNA expression in the livers of GalN/LPS-treated rats. LPZ also inhibited nuclear factor-kappa B activation by GalN/LPS.

Conclusions LPZ inhibits the induction of several inflammatory mediators (including cytokines, chemokines, and NO) partially through suppression of nuclear factor-kappa B, resulting in the prevention of fulminant liver failure. The therapeutic potential of LPZ for liver injuries warrants further investigation.

Keywords Primary cultured hepatocytes · Acute liver injury · Lansoprazole · D-galactosamine with lipopolysaccharide · Inducible nitric oxide synthase · Nuclear factor-kappa B

Richi Nakatake and Hidehiko Hishikawa contributed equally to this study.

✉ Richi Nakatake
nakatakr@hirakata.kmu.ac.jp

Hidehiko Hishikawa
auss0211@gmail.com

Masaya Kotsuka
kotsukam@hirakata.kmu.ac.jp

Morihiko Ishizaki
ishizakm@hirakata.kmu.ac.jp

Kosuke Matsui
matsuik@hirakata.kmu.ac.jp

Mikio Nishizawa
nishizaw@sk.ritsumei.ac.jp

Katsuhiko Yoshizawa
yoshizak@hirakata.kmu.ac.jp

Masaki Kaibori
kaibori@hirakata.kmu.ac.jp

Tadayoshi Okumura
okumura@hirakata.kmu.ac.jp

[1] Department of Surgery, Kansai Medical University, 2-5-1 Shinmachi, Hirakata, Osaka 573-1010, Japan

[2] Department of Biomedical Sciences, College of Life Sciences, Ritsumeikan University, 1-1-1 Nojihigashi, Kusatsu, Shiga 525-8577, Japan

[3] Laboratory of Environmental Sciences, Department of Food Sciences and Nutrition, School of Human Environmental Sciences, Mukogawa Women's University, 6-46 Ikebiraki-cho, Nishinomiya, Hyogo 663-8558, Japan

[4] Research Organization of Science and Technology, Ritsumeikan University, 1-1-1 Nojihigashi, Kusatsu, Shiga 525-8577, Japan

Introduction

Lansoprazole (LPZ) is a proton pump inhibitor that is used clinically to prevent and treat various acid-related diseases, including gastroesophageal reflux disease and peptic ulcers [1, 2]. The pharmacological effect of this drug is achieved by inhibiting hydrogen potassium adenosine triphosphatase, which in turn reduces gastric acid secretion from parietal cells.

In addition to its anti-secretory properties, LPZ is reported to have anti-inflammatory and anti-bacterial effects, and it has been used to treat *Helicobacter pylori* infections [3]. LPZ-induced mediation of inflammatory responses may occur partially through upregulation of heme oxygenase-1 in gastric mucosal cells [4] and the small intestine [5]. Researchers have proposed other mechanisms by which LPZ and other proton pump inhibitors exert anti-inflammatory effects [6–15]. For example, LPZ was found to suppress tumor necrosis factor alpha (TNF-α) and interleukin 1 beta (IL-1β) production in a human monocytic cell line that was induced by lipopolysaccharide (LPS) and *H. pylori* extracts through inhibiting nuclear factor-kappa B (NF-κB) and extracellular signal-regulated kinase signaling pathways [16]. LPZ may also have hepatoprotective effects because of its ability to induce an anti-oxidative stress response in the liver [17]. However, few studies have examined if LPZ administration influences survival in animal models of liver injury.

Excessive nitric oxide (NO) production by inducible nitric oxide synthase (iNOS) contributes to liver injury [18, 19]. In animal models of acute liver injury (induced by ischemia/reperfusion, partial hepatectomy, or endotoxin shock), drugs with hepatoprotective effects (e.g., pirfenidone [20], edaravone [21], and FR183998 [22, 23]) were shown to inhibit iNOS induction and NO production, as well as reduce the synthesis of proinflammatory mediators such as TNF-α, IL-1β, IL-6, and cytokine-induced neutrophil chemoattractant 1/chemokine (C-X-C motif) ligand 1 (CINC-1/CXCL-1; the rat analog of human IL-8). These drugs [22, 24, 25] were also shown to inhibit iNOS induction and NO production in primary rat hepatocyte cultures that are stimulated by IL-1β [26, 27]. Therefore, preventing iNOS induction and NO production may be considered to be indicators of hepatoprotection in hepatocyte cultures and animal models.

In this study, we examined the hepatoprotective effects of LPZ in in vitro and in vivo models. We first examined if LPZ inhibits iNOS induction and NO production in a primary cell culture of IL-1β-stimulated rat hepatocytes (representing an in vitro model of liver injury [28]) and the possible mechanisms behind these hepatoprotective effects. Next, we used an in vivo rat model of liver injury induced with D-galactosamine hydrochloride and LPS (GalN/LPS) to examine if LPZ influences rat survival.

Materials and Methods

Materials

LPZ was purchased from Takeda Pharmaceutical Co. Ltd. (Osaka, Japan), and recombinant human IL-1β (2×10^7 U/mg protein) was obtained from MyBioSource, Inc. (San Diego, CA, USA). GalN and LPS (*Escherichia coli* 0111: B4) were purchased from Wako Pure Chemical Corp. (Osaka, Japan) and Sigma-Aldrich Corp. (Saint Louis, MO, USA), respectively.

Male Wistar and Sprague–Dawley rats were obtained from Charles River Laboratories, Inc. (Tokyo, Japan). The rats were housed at 22 °C on a 12-h light/dark cycle for ≥ 7 days to allow acclimatization before experiments were conducted. Food and water were provided ad libitum. Animal care and experiments were performed in accordance with the standards outlined in the ARRIVE [29] and PREPARE [30] guidelines. The study protocol was approved by the Animal Care Committee at Kansai Medical University (Osaka, Japan) (Approval no. X18-027(1)).

Primary Rat Hepatocyte Culture Preparation

Collagenase perfusion was used to isolate hepatocytes from male Wistar rats (200–250 g; 6–7 weeks old) (Wako Pure Chemical Corp.) [31, 32]. The isolated hepatocytes were suspended in Williams' medium E at 6×10^5 cells/mL, seeded onto 35-mm plastic dishes (2 mL/dish; Falcon Plastics, Oxnard, CA, USA), and incubated at 37 °C in a humidified chamber (5% CO_2). Williams' medium E was supplemented with 10% newborn calf serum, HEPES (5 mmol/L), penicillin (100 U/mL), streptomycin (100 µg/mL), amphotericin B (0.25 µg/mL), aprotinin (0.1 µg/mL; Roche, Basel, Switzerland), dexamethasone (10 nmol/L), and insulin (10 nmol/L). After 2 h, the medium was replaced with fresh serum-free Williams' medium E (1.5 mL/dish). After another 5 h, the medium was again replaced with fresh serum- and hormone-free Williams' medium E (1.5 mL/dish), and the cells were cultured overnight before use. The number of cells attached to the dishes was estimated by counting the number of nuclei [33] and applying a ratio of 1.37 ± 0.04 nuclei/cell (mean ± standard error; $n=7$ experiments).

Induction of Acute Liver Injury in Rats

To induce acute liver injury for the in vivo model, male Sprague–Dawley rats (240–260 g; 7 weeks old) were anesthetized with isoflurane (Abbott Laboratories, Abbott Park,

IL, USA) before receiving an intravenous (i.v.) injection of GalN/LPS (500 mg/kg GalN and 50 μg/kg LPS) via the penile vein [34]. The rats that were randomly assigned to receive LPZ were injected (intraperitoneally, i.p.) with one of three LPZ doses (50, 100, or 200 mg/kg) 1 h before GalN/LPS treatment. Survival was monitored for 72 h after GalN/LPS injection. The rats were euthanized when they appeared weak and moribund as liver failure, congestion, and multiorgan failure progressed. We used the NIH Office of Animal Care and Use [35] score and severity assessment to assess the animals following liver resection [36]. Liver and blood samples were collected from the rats after 1 h and 6 h.

Treatment of the Cultured Hepatocytes with LPZ

LPZ was first dissolved in Williams' medium E and sterilized using a 0.45-μm membrane filter (Millipore, Billerica, MA, USA). On the day after cell culture, the hepatocytes were washed with fresh serum- and hormone-free Williams' medium E and incubated with IL-1β (1 nmol/L) in the same medium either in the presence or absence of LPZ (dose range, 25–250 μM).

Determination of NO Production and Lactate Dehydrogenase Activity in the Cultured Hepatocytes

The amount of nitrite (a stable metabolite of NO) in the cell culture medium of the hepatocytes was measured using the Griess method [37]. Cell viability was measured based on lactate dehydrogenase activity using a commercial kit (Roche Diagnostics, Risch-Rotkreuz, Switzerland).

Western Blot Analysis

Total cell lysates were obtained from the cultured hepatocytes using a previously described method with minor modifications [24]. Briefly, cells (1×10^6 cells/35-mm dish) were lysed with sample buffer (125 mmol/L Tris–HCl, pH 6.8; containing 5% glycerol, 2% SDS, and 1% 2-mercaptoethanol), and protein levels were examined using sodium dodecyl sulfate–polyacrylamide gel electrophoresis (SDS-PAGE). Frozen liver samples were homogenized in five volumes of cell solubilization buffer (10 mmol/L Tris–HCl, pH 7.4; containing 1% Triton X-100, 0.5% Nonidet P-40, 1 mmol/L ethylenediaminetetraacetic acid [EDTA], 1 mmol/L ethylene glycol-bis[2-aminoethyl ether] tetraacetic acid, and 150 mmol/L NaCl) with 1 mmol/L phenylmethylsulfonylfluoride (PMSF) and cOmplete™ protease inhibitor cocktail (1×; Roche Diagnostics) before centrifugation at 16,500*g* for 15 min at room temperature. The supernatants were mixed with SDS-PAGE sample buffer (2×). SDS-PAGE was then performed and the separated proteins were electroblotted onto polyvinylidene difluoride membranes (Bio-Rad Laboratories, Hercules, CA, USA). Immunostaining was performed using primary antibodies for mouse iNOS (Affinity BioReagents, Golden, CO, USA), human inhibitor of κB alpha (IκBα; Santa Cruz Biotechnology, Santa Cruz, CA, USA), mouse type-I IL-1 receptor (IL-1RI; Santa Cruz Biotechnology), and rat β-tubulin (internal control; Clone TUB2.1; Sigma-Aldrich Corp.). Immunoreactive proteins were visualized using an enhanced chemiluminescence detection kit (GE Healthcare Biosciences, Piscataway, NJ, USA).

To measure the levels of protein kinase B (Akt) in the cultured hepatocytes, total cell lysates from 100-mm dishes (5×10^6 cells/dish) were prepared with a cell solubilization buffer containing 1 mmol/L PMSF, cOmplete™ protease inhibitor cocktail (1×; Roche Diagnostics), and phosphatase inhibitor cocktail (1×; Nacalai Tesque Inc., Kyoto, Japan). The extracts were pre-cleared with protein A (Sigma-Aldrich Corp.) and mixed with a mouse monoclonal antibody for human Akt1 (Akt5G3; Cell Signaling Technology Inc., Beverly, MA, USA) and protein G-Sepharose beads (Pharmacia LKB Biotech, Uppsala, Sweden). After overnight incubation at 4 °C, the immune complexes were centrifuged at 16,000*g* for 5 min at room temperature. The beads were washed with solubilization buffer, dissolved in SDS-PAGE sample buffer, and analyzed using western blot (SDS-PAGE in 10% gel) with rabbit polyclonal antibodies for human Akt and phospho-Akt (Ser473) (Cell Signaling Technology Inc.) as the primary antibodies.

Reverse Transcriptase Polymerase Chain Reaction

Total RNA was extracted from the cultured hepatocytes or frozen liver samples using TRIzol® reagent (Sigma-Aldrich Corp.) and a guanidinium thiocyanate-phenol–chloroform mixture [38]. For strand-specific reverse transcriptase polymerase chain reaction (RT-PCR), cDNA was first synthesized from total RNA with strand-specific primers; touchdown PCR was then performed using a PC-708 thermal cycler (Astec Co. Ltd., Fukuoka, Japan) based on a previously described method with minor modifications [39]. We examined iNOS (257 bp), TNF-α (275 bp), CXCL-1 (231 bp), IL1RI (327 bp), IL-1β (321 bp), IL-6 (286 bp), IL-10 (245 bp), and elongation factor 1 alpha (EF-1α; internal control; 335 bp) mRNA expression using an oligo (dT) primer and the relevant primer sets (Table 1). The mRNA levels were measured using real-time PCR on a Rotor-Gene Q 2plex HRM platform (QIAGEN, Tokyo, Japan). A Rotor-Gene SYBR™ Green PCR kit (QIAGEN) was used in the reaction mixture, and the following touchdown PCR protocol was used: 1 cycle at 95 °C for 5 min, 45 cycles at 95 °C for 5 s, and 60 °C for 10 s. The cDNA sequence for rat iNOS mRNA was deposited in the DNA Data Bank of

Table 1 List of RT-PCR primer sets

Primer name	Nucleotide sequence
iNOS F/R	5′-CCAACCTGCAGGTCTTCGATG-3′/5′-GTCGATGCACAACTGGGTGAAC-3′
TNF-α F/R	5′-TCCCAACAAGGAGGAGAAGTTCC-3′/5′-GGCAGCCTTGTCCCTTGAAGAGA-3′
CINC-1/CXCL-1 F/R	5′-GCCAAGCCACAGGGGCGCCCGT-3′/5′-ACTTGGGGACACCCTTTAGCATC-3′
IL-1β F/R	5′-TCTTTGAAGAAGAGCCCGTCCTC-3′/5′-GGATCCACACTCTCCAGCTGCA-3′
IL-6 F/R	5′-GAGAAAAGAGTTGTGCAATGGCA-3′/5′-TGAGTCTTTTATCTCTTGTTTGAAG-3′
IL-10	5′-GCAGGACTTTAAGGGTTACTTGG-3′/5′-CCTTTGTCTTGGAGCTTATTAAA-3′
EF F/R	5′-TCTGGTTGGAATGGTGACAACATGC-3′/5′-CCAGGAAGAGCTTCACTCAAAGCTT-3′

iNOS inducible nitric oxide synthase; *TNF-α* tumor necrosis factor-α; *CINC-1/CXCL-1* cytokine-induced neutrophil chemoattractant-1/chemokine (C-X-C motif) ligand 1; *IL-1β* interleukin-1β; *IL-6* interleukin-6; *IL-10* interleukin-10; *EF* elongation factor-1α. *F/R* forward/reverse

Japan/European Bioinformatics Institute/GenBank under accession number AB250951.

Electrophoretic Mobility Shift Assay

Nuclear extracts were prepared from the cultured hepatocytes or frozen liver samples, and an electrophoretic mobility shift assay was performed using a previously described method [40]. Liver Sects. (0.1 g) from frozen liver samples were homogenized using a Dounce homogenizer (Sigma-Aldrich Corp.) in 2 mL of buffer A (10 mmol/L HEPES–KOH, pH 7.9; containing 10 mmol/L KCl, 1.5 mmol/L $MgCl_2$, 1 mmol/L dithiothreitol, 1 mmol/L PMSF, and 5 μg/mL aprotinin), allowed to stand for 15 min, and centrifuged at 1100*g* for 5 min at 4 °C. The pellets obtained were then suspended in 1 mL of lysis buffer (buffer A supplemented with 0.1% Triton X-100), allowed to stand for 10 min, and centrifuged at 1100*g* for 10 min at 4 °C. The nuclear pellets were then suspended in 80 μL of nuclear extraction buffer (20 mmol/L HEPES–KOH, pH 7.9; containing 0.42 M NaCl, 1.5 mmol/L $MgCl_2$, 1 mmol/L dithiothreitol, 1 mmol/L PMSF, 5 μg/mL aprotinin, 0.2 mmol/L EDTA, and 25% [*v/v*] glycerol), incubated for 30 min, and centrifuged at 16,500*g* for 20 min at 4 °C.

The binding reactions (total mixture, 15 μL) were performed by incubating the nuclear extracts in reaction buffer (20 mmol/L HEPES–KOH, pH 7.9; containing 1 mmol/L EDTA, 60 mmol/L KCl, 10% glycerol, and 1 μg poly[dI-dC]) with a double-stranded DNA probe (40,000 dpm) for 20 min at room temperature. The products were electrophoresed using a 4.8% polyacrylamide gel in high ionic strength buffer, and autoradiography was used to analyze the dried gels. An NF-κB consensus oligonucleotide (sense strand: 5′-AGTTGAGGGGA-CTTTCCCAGGC) produced from a mouse immunoglobulin light-chain mRNA was purchased from Promega Corp. (Madison, WI, USA). To produce the double-stranded DNA probe, oligonucleotides containing a κB site were labeled with [γ-^{32}P]-adenosine-5′-triphosphate (DuPont-New England Nuclear Japan, Tokyo, Japan) and T4 polynucleotide kinase (Takara Biotechnology, Kyoto, Japan). Protein concentrations were measured using a binding assay kit (Bio-Rad Laboratories); the Bradford method [41] was employed with bovine serum albumin as the standard.

Transfection and Luciferase Assay of the Cultured Hepatocytes

Transfection of the cultured hepatocytes was performed using a previously described method [42]. Hepatocytes were cultured at 3×10^5 cells/dish (35 × 10 mm) in Williams' medium E with serum, dexamethasone, and insulin for 7 h before undergoing magnet-assisted transfection. Reporter constructs pRiNOS-Luc-SVpA (for detecting the transactivation of the iNOS promoter) or pRiNOS-Luc-3′UTR (for detecting the stability of mRNA) (1 μg) and the cytomegalovirus promoter-driven β-galactosidase plasmid pCMV-LacZ (1 ng; internal control) were mixed with a magnet-assisted transfection reagent (1 μL; IBA Lifesciences, Göttingen, Germany) in fresh serum- and hormone-free Williams' medium E (1 mL/dish). Following a 15-min incubation period on a magnetic plate at room temperature, the medium was replaced with fresh Williams' medium E with serum. The cells were then cultured overnight and treated with IL-1β either in the presence or absence of LPZ. Luciferase and β-galactosidase activities in the resulting cell extracts were measured using a PicaGene kit (Wako Pure Chemical Corp.) and Beta-Glo kit (Promega), respectively.

Histopathological Analysis of the Rat Model

Excised liver specimens from the Sprague–Dawley rats collected 1 h and 6 h after GalN/LPS treatment were fixed in 4% formalin and embedded in paraffin. Sections of 3–5 μm in size were cut and stained with hematoxylin and eosin (H&E). Apoptotic bodies in the hepatocyte nuclei were detected by terminal deoxynucleotidyl transferase-mediated deoxyuridine triphosphate-digoxigenin nick-end

labeling (TUNEL) staining using an apoptosis detection kit purchased from Medical and Biological Laboratories Co. Ltd. (Nagoya, Japan). Neutrophil infiltration was evaluated by staining with myeloperoxidase (MPO) using anti-MPO antibodies (rabbit polyclonal; Dako, Carpinteria, CA, USA) before H&E staining. The number of TUNEL- and MPO-positive cells per square millimeter was counted by analysts who were blinded to the treatment arm.

Serum Biochemical Analysis of the Rat Model

Blood samples from the Sprague–Dawley rats were collected 1 h and 6 h after GalN/LPS treatment. Serum aspartate transaminase (AST) and alanine transaminase (ALT) levels were quantified using commercial kits (Wako Pure Chemical Corp.). The serum levels of nitrite and nitrate (stable metabolites of NO) were also measured using a commercial kit (Roche, Mannheim, Germany) based on the Griess method [37].

Statistical Analyses

Quantitative results were obtained from three to four independent experiments for each of the various analyses, and the mean values and their standard deviations were calculated. Differences between groups and in survival were identified using the Student's *t* test and log-rank test, respectively. $P < 0.05$ was considered significant.

Results

LPZ Inhibits iNOS Induction and NO Production in Cultured Hepatocytes

IL-1β stimulates iNOS protein expression and NO production in primary rat hepatocyte cultures [26]. However, our experiments showed that simultaneously adding LPZ and IL-1β decreased NO production in a time-dependent (Fig. 1a) and dose-dependent manner (Fig. 1b, upper panel). Higher LPZ doses continued to reduce iNOS protein expression (Fig. 1b, middle panel), and inhibited over 80% of iNOS protein expression and NO production at a dose of 250 μM (92 μg/mL). LPZ showed no cellular toxicity at the indicated concentrations, as evaluated by lactate dehydrogenase release and trypan blue exclusion (data not shown). Real-time PCR showed that LPZ decreased iNOS, TNF-α [43], and CXCL-1 [44] mRNA expression (Fig. 1c–e), indicating that LPZ affects these genes at the transcriptional and/or post-transcriptional levels.

LPZ Decreases iNOS mRNA Synthesis and Reduces Its Stability in the Cultured Hepatocytes

iNOS mRNA expression is regulated through activation of the iNOS promoter by transcription factors such as NF-κB and through post-transcriptional modifications such as mRNA stabilization [45]. Transfection was performed using pRiNOS-Luc-SVpA and pRiNOS-Luc-3′ UTR, which detect iNOS promoter activation (i.e., mRNA synthesis) and mRNA stability, respectively [42]. IL-1β increased luciferase activity of these vector constructs, and this effect was significantly inhibited by LPZ (Fig. 2).

LPZ Blocks IκB/NF-κB Signaling in Cultured Hepatocytes

iNOS induction is mediated by two main signaling pathways: IκB kinase and phosphatidylinositol 3-kinase/Akt [46]. IL-1β stimulates IκBα degradation via its phosphorylation by IκB kinase and subsequent NF-κB activation (causing nuclear translocation and DNA binding). As shown in Fig. 3, LPZ inhibited NF-κB activation, but had no effect on IκBα degradation.

LPZ Improves Survival in GalN/LPS-Treated Rats

GalN-induced liver damage in rats has similar metabolic and morphologic aberrations as that caused by human viral hepatitis [47]. GalN is often used in combination with LPS to produce an animal model of severe acute liver injury with almost 100% mortality.

In our rat model of acute liver injury, the GalN/LPS + LPZ (100 mg/kg) group (Fig. 4a, left panel, filled circles) showed a significant increase in survival (50%) compared with the GalN/LPS only group (open circles). Adverse effects were observed at an LPZ dose of 200 mg/kg body weight (Fig. 4b, right panel, filled triangles). AST and ALT serum levels were reduced upon treatment with LPZ (100 mg/kg) (Fig. 5a, b). The excessive production of NO driven by iNOS has an important role in hepatic dysfunction during endotoxemia. Serum levels of nitrite and nitrate increased after GalN/LPS treatment at 6 h; however, LPZ inhibited this increase (Fig. 5c).

LPZ Affects Hepatic iNOS Protein Expression and NF-κB Activation in GalN/LPS-Treated Rats

Similar to the results in the cultured hepatocytes, western blot analysis demonstrated that GalN/LPS treatment increased hepatic iNOS protein expression at 6 h, but LPZ reduced this expression (Fig. 6a). Electrophoretic mobility shift assay results also indicated that LPZ suppressed NF-κB activation by GalN/LPS at 6 h (Fig. 6b).

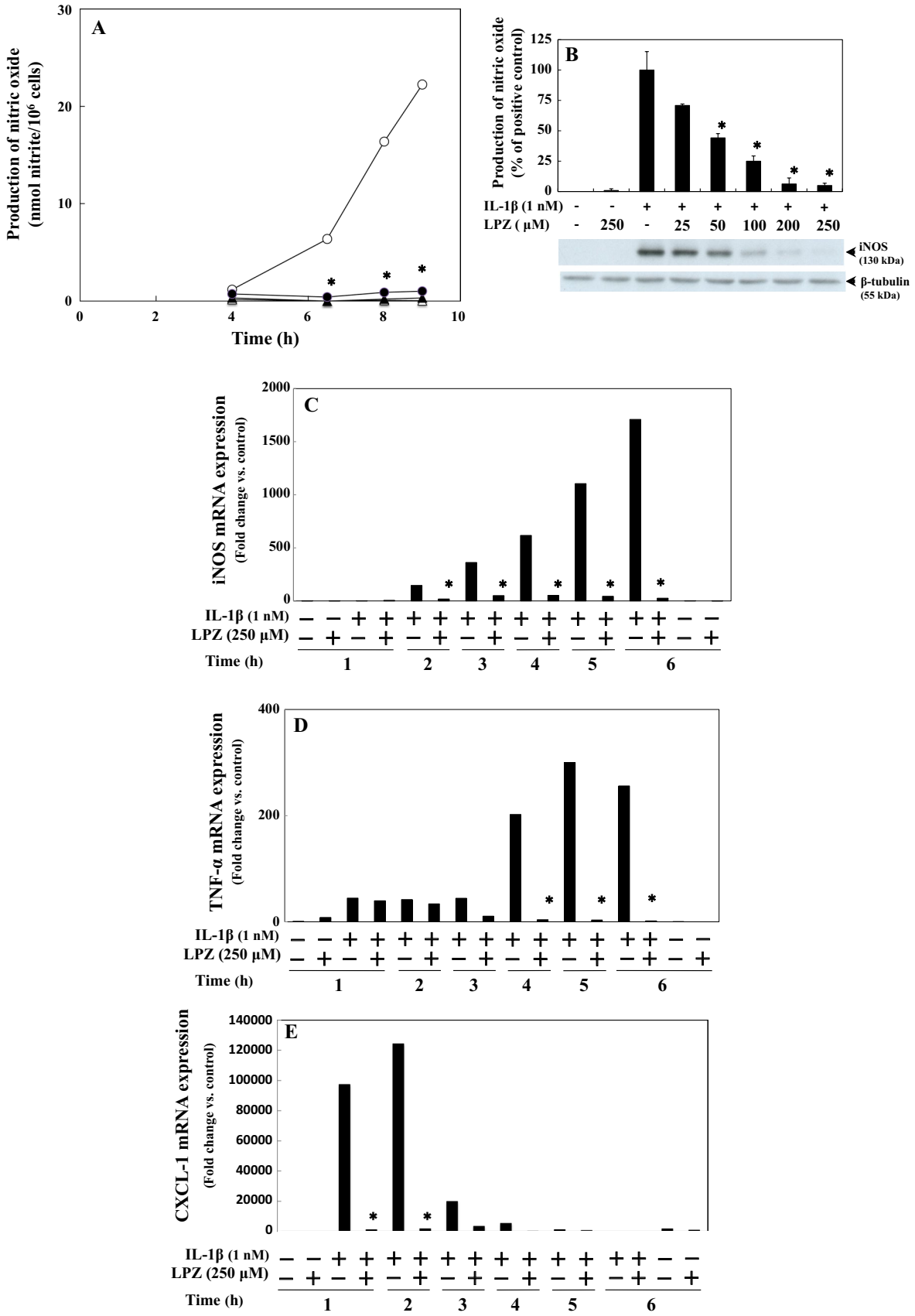
A
Production of nitric oxide (nmol nitrite/10^6 cells)
Time (h)
B
Production of nitric oxide (% of positive control)
IL-1β (1 nM)
LPZ (μM)
iNOS (130 kDa)
β-tubulin (55 kDa)
C
iNOS mRNA expression (Fold change vs. control)
IL-1β (1 nM)
LPZ (250 μM)
Time (h)
D
TNF-α mRNA expression (Fold change vs. control)
E
CXCL-1 mRNA expression (Fold change vs. control)

◂**Fig. 1** Effects of LPZ on the induction of NO, iNOS protein and mRNA, TNF-α mRNA, and CXCL-1 mRNA in IL-1β–stimulated hepatocytes. The cells were treated with IL-1β (1 nM) in the presence or absence of LPZ. **a** Effect of LPZ (250 μM) treatment for the indicated times on NO production (IL-1β, open circles; IL-1β + LPZ, filled circles; LPZ, filled triangles; controls without IL-1β or LPZ, open triangles). **b** Effect of 8-h treatment with LPZ (25–250 μM) on NO production (upper panel) and iNOS protein levels (middle panel). Nitrite levels were measured in the culture medium. The values in the bar graphs represent the mean ± standard deviation ($n = 3$ dishes per time-point). *$P < 0.05$ versus IL-1β alone. In the western blot panels, cell lysates (20 μg of protein) were subjected to SDS-PAGE in a 7.5% gel and immunoblotted with anti-iNOS or anti-β-tubulin antibodies. **c**–**e** The cells were treated with IL-1β (1 nM) in the presence or absence of LPZ (250 μM) for the indicated times. Total RNA was analyzed with strand-specific RT-PCR to detect **c** iNOS mRNA, **d** TNF-α mRNA, and **e** CXCL-1 mRNA using EF-1α mRNA as the internal control

LPZ Decreases Hepatic iNOS mRNA and Proinflammatory Mediator Expression in GalN/LPS-Treated Rats

Although GalN/LPS treatment increased hepatic iNOS mRNA expression in GalN/LPS-treated rats, LPZ inhibited its expression at 6 h (Fig. 7a). The GalN/LPS + LPZ group also had lower TNF-α (1 h), CXCL-1 (1 h), IL-1β (6 h), and IL-6 (1 and 6 h) mRNA expression (Fig. 7b–e). However, LPZ increased mRNA expression of the anti-inflammatory cytokine IL-10 at 1 h (Fig. 7f), but GalN/LPS treatment had no significant effect on its expression.

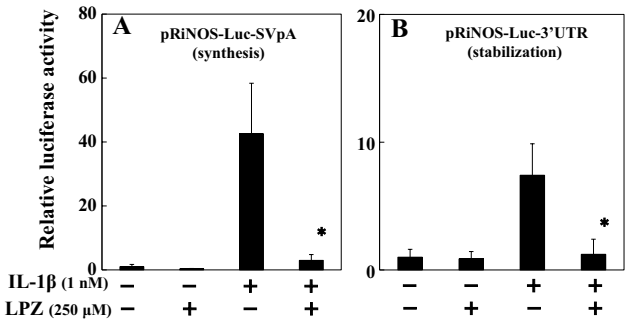

Fig. 2 Effects of LPZ on iNOS promoter transactivation and iNOS mRNA stability in IL-1β-stimulated hepatocytes. Two reporter constructs consisting of the rat iNOS promoter (1.0 kb), a luciferase gene, and the SV40 poly(A) region (pRiNOS-Luc-SVpA) or iNOS 3′-UTR (pRiNOS-Luc-3′ UTR) were used for transfection. The iNOS 3′-UTR contains adenylate–uridylate-rich elements (AUUU(U)A × 6) that contribute to mRNA stabilization. Each construct was introduced into the hepatocytes, and the cells were treated with IL-1β (1 nM) in the presence or absence of LPZ (250 μM) for **a** 8 h with pRiNOS-Luc-SVpA or **b** 5 h with pRiNOS-Luc-3′ UTR. Luciferase activity was normalized by β-galactosidase activity. Fold activation was calculated by dividing luciferase activity by control activity (without IL-1β or LPZ). The values in the bar graphs represent the mean ± standard deviation ($n = 4$ dishes). *$P < 0.05$ versus IL-1β alone

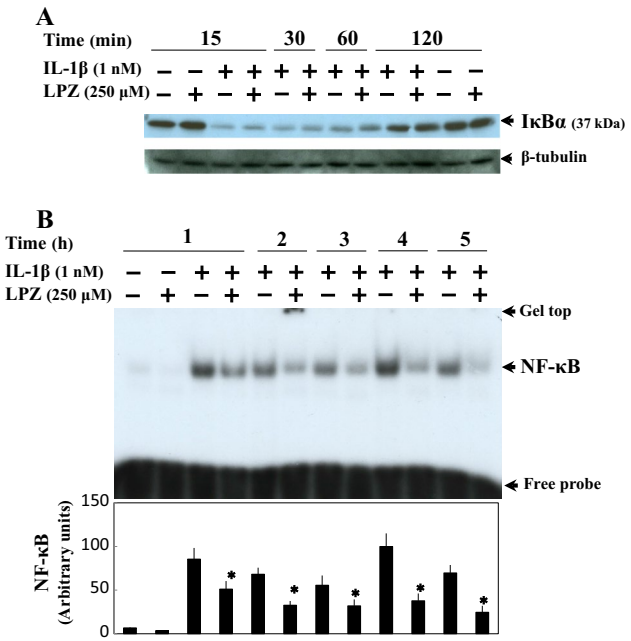

Fig. 3 Effects of LPZ on IκBα degradation and NF-κB activation in IL-1β-stimulated hepatocytes. Cells were treated with IL-1β (1 nM) in the presence or absence of LPZ (250 μM) for the indicated times. **a** To examine IκBα degradation, cell lysates (20 μg of protein) were subjected to SDS-PAGE in a 12.5% gel and immunoblotted with anti-IκBα or anti-β-tubulin antibodies. **b** To examine NF-κB activation, nuclear extracts (4 μg of protein) were analyzed using an electrophoretic mobility shift assay. The representative results of three independent experiments are shown. The NF-κB bands were quantified using densitometry. The values in the bar graph represent the mean ± standard deviation ($n = 3$ experiments). *$P < 0.05$ versus IL-1β alone

LPZ Decreases Hepatic Apoptosis and Necrosis in GalN/LPS-Treated Rats

The livers of GalN/LPS-treated rats were histologically examined 1 h and 6 h after GalN/LPS injection. Representative images of the H&E-stained liver sections are shown in Fig. 8a–d. Liver damage was characterized by inflammatory cell infiltration, hemorrhagic manifestations, and focal necrosis (Fig. 8c). Focal necrosis with hemorrhagic manifestations and ballooning degeneration were also observed in the hepatocytes. However, LPZ reduced the incidence and extent of these pathological changes (Fig. 8d). Representative images of liver sections that were immunostained with anti-TUNEL antibodies are shown in Fig. 8e–h. GalN/LPS increased apoptosis in the hepatocytes (Fig. 8g), whereas LPZ markedly decreased apoptosis (Fig. 8h). Quantifying the number of apoptotic cells in the microscopic fields revealed that LPZ significantly decreased ($P < 0.01$) the liver apoptotic index (Fig. 8i). Representative images of liver sections immunostained with anti-MPO antibodies are shown in Fig. 8j–m. GalN/LPS markedly increased

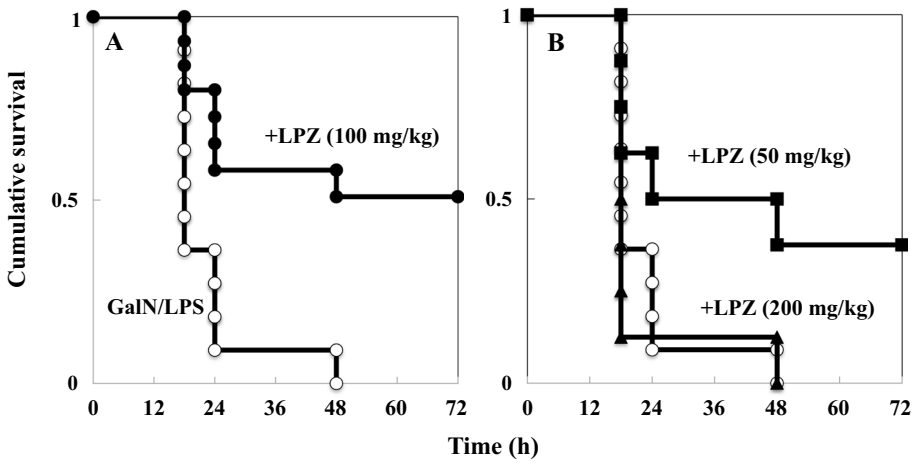

Fig. 4 Effects of LPZ on GalN/LPS-treated rat survival. LPZ (50–200 mg/kg) was administered (i.p.) 1 h before GalN/LPS treatment. Kaplan–Meier survival curves represent the cumulative survival of the following treatment groups: GalN/LPS only (positive control; **a**, **b** open circles,), GalN/LPS + LPZ (50 mg/kg; **b**, filled squares), GalN/LPS + LPZ (100 mg/kg; **a**, filled circles), and GalN/LPS + LPZ (200 mg/kg; **b**, filled triangles). The values represent the percentage of survival at the indicated times after GalN/LPS treatment (8–15 rats/group). $*P < 0.05$ versus GalN/LPS only rats

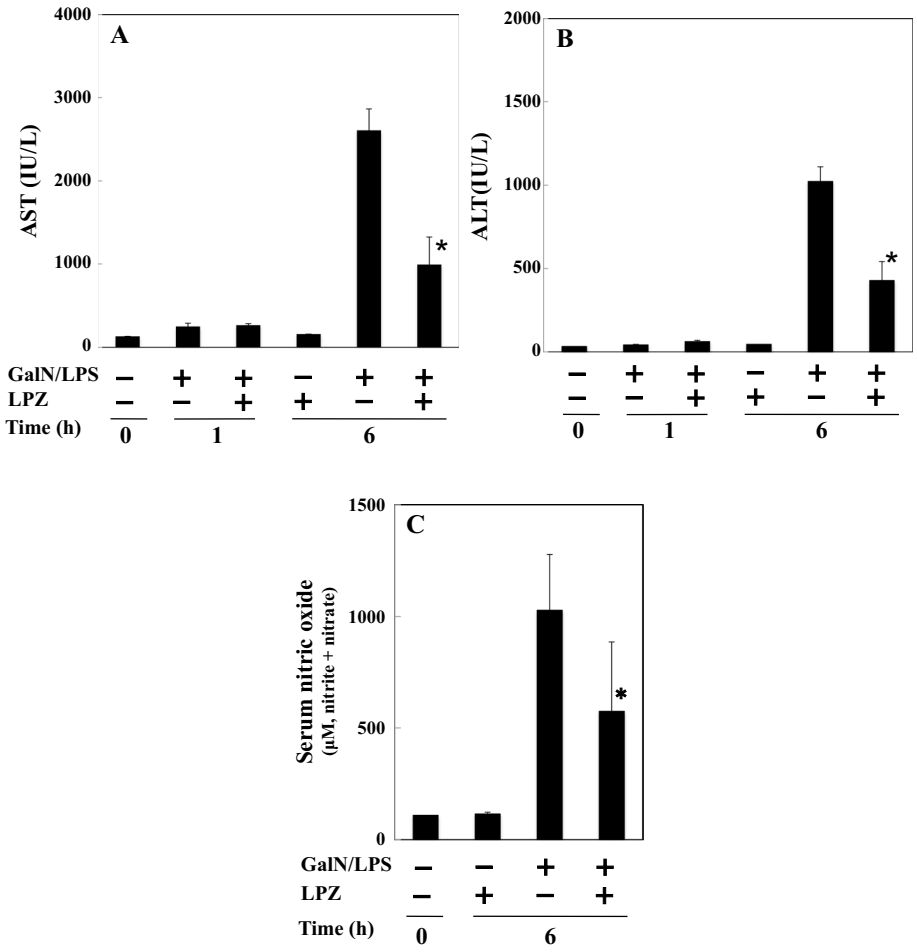

Fig. 5 Effects of LPZ on serum AST, ALT, and NO levels in GalN/LPS-treated rats. LPZ (100 mg/kg) was administered (i.p.) 1 h before GalN/LPS treatment. Blood samples were collected at the indicated times after GalN/LPS treatment. The levels of **a** AST, **b** ALT, and **c** NO_2^- and NO_3^- (metabolites of nitric oxide) were measured. The values in the bar graphs represent the mean ± standard error ($n = 5$ rats per time-point per group). $*P < 0.05$ versus GalN/LPS only rats

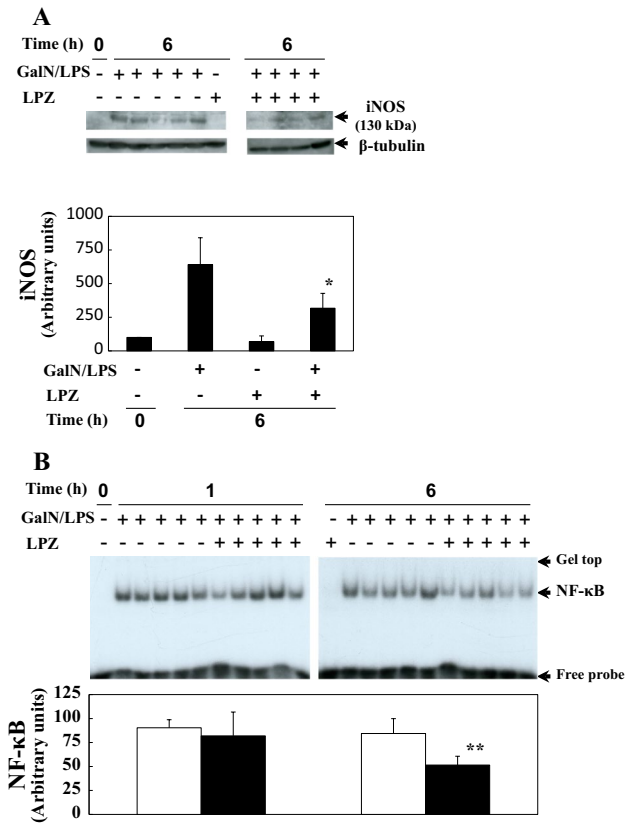

Fig. 6 Effects of LPZ on hepatic iNOS induction and NF-kB activation in GalN/LPS-treated rats. LPZ (100 mg/kg) was administered (i.p.) 1 h before GalN/LPS treatment. **a** For western blot analysis, liver samples were obtained 6 h after GalN/LPS treatment. Cell lysates (150 µg protein) were subjected to SDS-PAGE in a 7.5% gel and immunoblotted with anti-iNOS (upper band) or anti-β-tubulin (lower band) antibodies. The representative results of two independent experiments are shown. The iNOS bands were quantified using densitometry (lower panel; $n=4$–5 experiments). **b** Nuclear extracts (4 µg of protein) were prepared from the liver at the indicated times after GalN/LPS treatment, and NF-kB was analyzed using an electrophoretic mobility shift assay (upper panel). The NF-kB bands were quantified using densitometry (lower panel; $n=5$ experiments). The values in the bar graphs represent the mean ± standard error. *$P<0.05$ and **$P<0.01$ versus GalN/LPS only rats

hepatocyte necrosis (Fig. 8l). LPZ significantly decreased ($P<0.05$) number of MPO-positive cells in the microscopic fields (Fig. 8n). These images suggest that LPZ reduced liver injury caused by hepatocyte apoptosis and necrosis.

Discussion

Mortality caused by sepsis is high despite current treatments, even when the species of the infected bacteria is identified. Sepsis progression is classified as early (warm shock, i.e., hyperdynamic state with peripheral vasodilation) and late (cold shock, i.e., hypodynamic state without efficient peripheral circulation). Excess NO is assumed to be a dominant vasodilator in warm shock and triggers secondary responses, including multiple organ failure, in cold shock [48]. Sepsis in the endotoxemia rat model is divided into two phases, including warm shock (0–3 h after the LPS injection) and cold shock (6 h or more after the LPS injection). Therefore, we administered LPZ 1 h before GalN/LPS treatment to monitor the survival rate and apoptosis in the liver by inhibiting hepatic iNOS expression and NO production during warm shock.

In this study, we investigated the hepatoprotective effects of LPZ using IL-1β-stimulated rat hepatocytes and GalN/LPS-treated rats as in vitro and in vivo liver injury models, respectively. LPZ demonstrated hepatoprotective effects in both types of models, and our experiments indicated several possible mechanisms for these effects.

Upregulation of iNOS, TNF-α, and other proinflammatory cytokines in inflamed hepatocytes is central to liver inflammation. In response to interactions with pathogenic bacteria, inflammatory cells increase production of these cytokines, which in turn activate other processes that promote inflammation. Tanigawa et al. reported that LPZ inhibits TNF-α and IL-1β production in a THP-1 monocytic cell line stimulated by LPS or an *H. pylori* extract [16]. Nakamura et al. [49] observed LPZ uptake in polymorphonuclear cells and macrophages in the colonic mucosa of colitic rats. These findings suggest that LPZ may exert anti-inflammatory effects in bacteria-induced gastrointestinal inflammation via the suppression of proinflammatory cytokine production in inflammatory cells.

We found that LPZ suppressed iNOS induction and NO production in cultured hepatocytes (Fig. 1) partially through inhibiting NF-κB activation (Fig. 3). iNOS mRNA levels were reduced by inhibiting mRNA synthesis and reducing its stability (Fig. 2). LPZ also decreased TNF-α and CXCL-1 mRNA levels (Fig. 1), indicating that the hepatoprotective effects were also exerted by inhibiting proinflammatory cytokine expression. These findings are consistent with the results of previous studies [16, 49]. In our rat model of acute liver injury, LPZ reduced the appearance of pathologic changes such as apoptosis and necrosis (Fig. 8) and attenuated the serum AST and ALT levels (Fig. 5). This led to a marked improvement in rat survival (Fig. 4).

LPS has been reported to stimulate Kupffer cells in rat livers via toll-like receptor 4 (TLR4) to produce proinflammatory cytokines, which then induce hepatic infiltration of neutrophils [50]. In our study, LPZ was observed to inhibit hepatic iNOS, TNF-α, CXCL-1, IL-1β, and IL-6 mRNA expression in GalN/LPS-treated rats (Fig. 7), indicating that LPZ prevented the expression of these proinflammatory mediators at the transcriptional level. The earliest events following LPS stimulation through TLR4 activate NF-κB

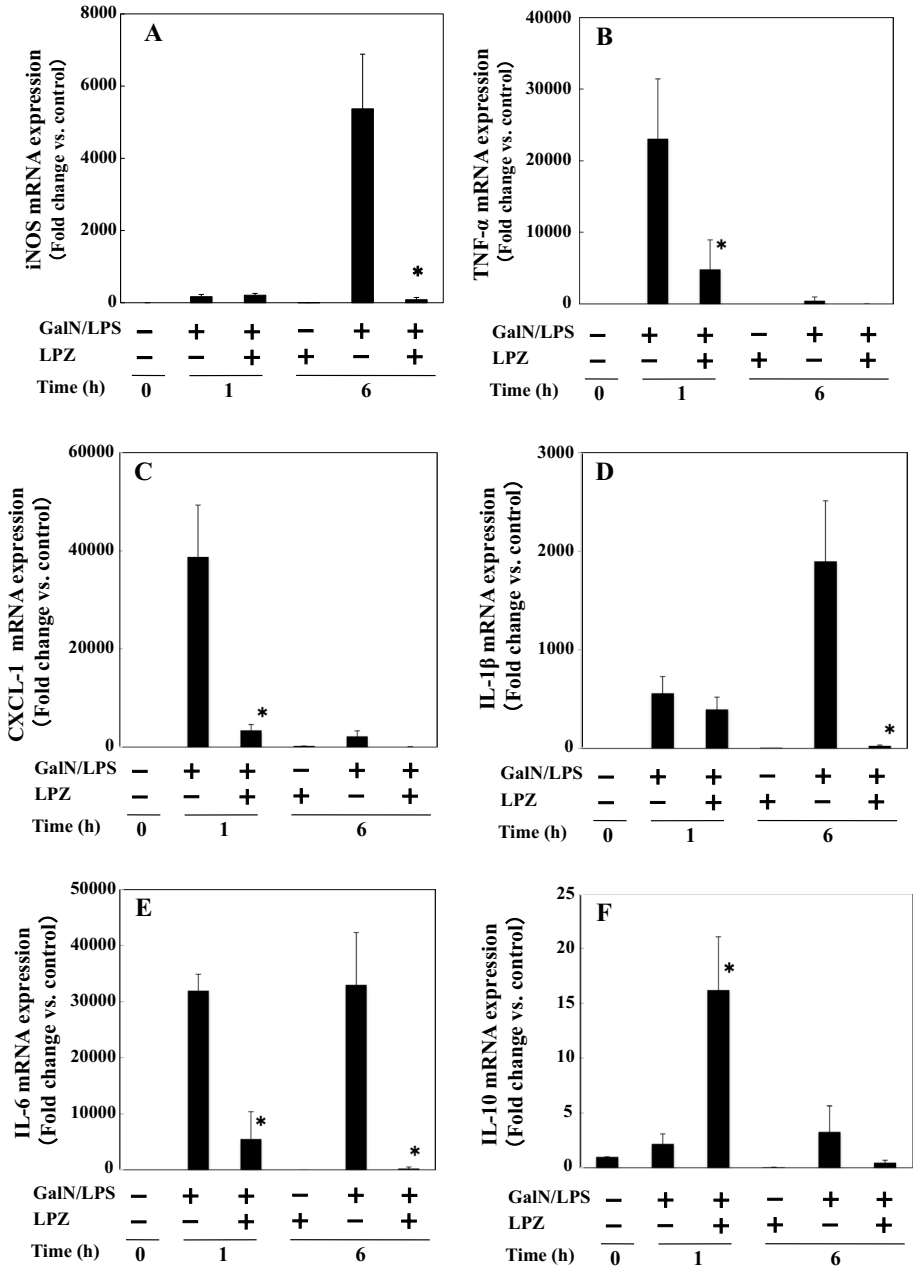

Fig. 7 Effects of LPZ on iNOS and proinflammatory cytokine mRNA expression in the livers of GalN/LPS-treated rats. LPZ (100 mg/kg) was administered (i.p.) 1 h before GalN/LPS treatment. Total RNA was extracted from the liver at the indicated times after GalN/LPS treatment and analyzed using strand-specific real-time RT-PCR to detect **a** iNOS, **b** TNF-α, **c** CXCL-1, **d** IL-1β, **e** IL-6, and **f** IL-10 mRNA expression. The data were calculated as the fold-change versus GalN/LPS only rats (control group). The values in the bar graphs represent the mean ± standard error ($n = 5$ rats per time-point per group). *$P < 0.05$ versus GalN/LPS only rats

in cells, its translocation from the cytoplasm to the nucleus, and DNA binding [47]. In Kupffer cells, GalN increased LPS binding to TLR4, which promotes transcriptional upregulation of various proinflammatory mediators including TNF-α, CXCL-1, and iNOS [51–54].

The electrophoretic mobility shift assay of nuclear extracts from the liver revealed that LPZ decreased NF-κB by GalN/LPS activation (Fig. 6), which supports the observations described above. To minimize the number of animals used in the experiments, we chose sampling points and the minimum number of replicates required to detect statistical significance. Although the dose of LPZ (100 mg/kg) used in this study exceeds that of standard clinical use (0.6–1.2 mg/kg), this dose has been previously used in experimental studies involving rat models [55]. Our simple in vitro model (primary cultured rat hepatocytes) may be adequate for screening of liver-protective drugs, because it is rapid and inexpensive compared with animal models of liver injury. However, the doses used in the in vitro and even in vivo (animal model) experiments are relatively high compared with clinical use in humans, which is a limitation in these models. Thus, the liver-protective effects of high-dose drugs that are deduced using these models and their side effects need to be examined, confirmed, and supported

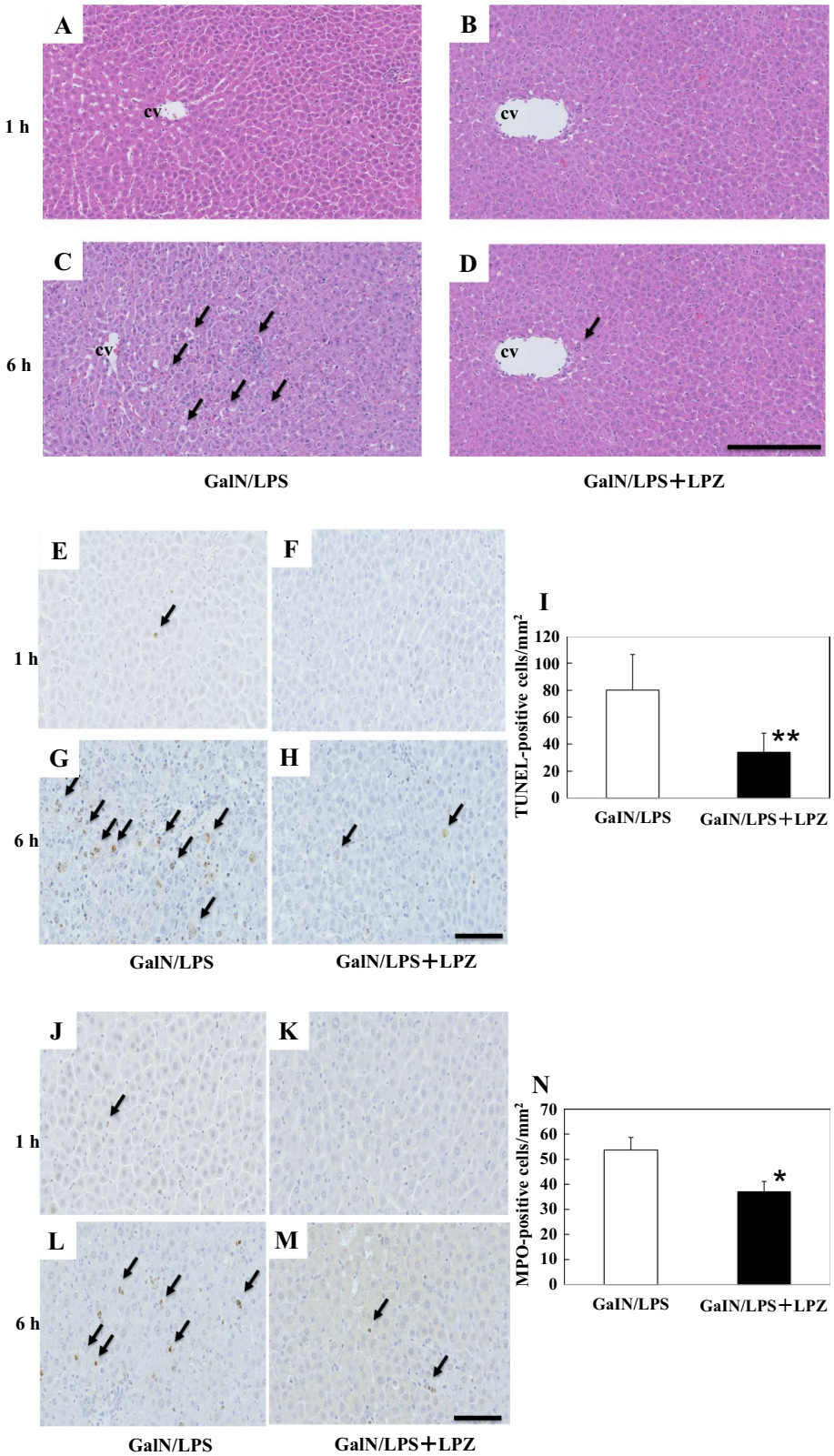

Fig. 8 Effects of LPZ on hepatic pathological changes in GalN/LPS-treated rats. LPZ (100 mg/kg) was administered (i.p.) 1 h before GalN/LPS treatment. **a**–**d** Histologic appearance of the liver after GalN/LPS treatment. Liver sections of rats treated with GalN/LPS (**a**, **c**) and GalN/LPS + LPZ (**b**, **d**) were obtained 1 h or 6 h after GalN/LPS treatment and stained with H&E (magnification × 200). Note the areas of focal necrosis with inflammatory cell infiltration and massive hemorrhage in GalN/LPS rats (cv, central vein; arrows, apoptosis; bar = 250 μm). **e**–**n** Effects of LPZ on apoptosis (**e**–**i**) and necrosis (**j**–**n**) in the liver. Liver sections of rats treated with GalN/LPS (**e**, **g**, **j**, **l**) and GalN/LPS + LPZ (**f**, **h**, **k**, **m**) were obtained 1 h or 6 h after GalN/LPS treatment and staining with TUNEL (**e**–**h**) or MPO (**j**–**m**) (magnification × 200). Note the brown nuclei in the positive cells (arrows, positive cells; bar = 100 microns). The numbers of **i** TUNEL-positive cells and **n** MPO-positive cells per square millimeter were counted. The values in the bar graphs represent the mean ± standard error ($n = 5$ rats per time-point per group). *$P < 0.05$ and **$P < 0.01$ versus GalN/LPS only rats

in humans. Llorente et al. [56] described that gastric acid suppression by proton pump inhibitor increases intestinal Enterococcus and promotes alcoholic liver disease. When using long time treatment of proton pump inhibitors, these side effects should be concerned to chronic liver inflammation and hepatocyte damage.

Conclusions

The appropriate regulation of inflammatory reactions during the perioperative period is important to prevent organ damage and complications from infection. In this study, we investigated the hepatoprotective effects of LPZ using in vitro and in vivo liver injury models. Our experiments showed that LPZ inhibits proinflammatory mediator expression (such as iNOS and TNF-α) by suppressing NF-κB activation. Additionally, LPZ was found to significantly increase survival in GalN/LPS-treated rats. These results suggest that LPZ may aid in preventing liver injury, and further in-depth studies are needed to explore its possible therapeutic applications.

Acknowledgments This work was supported in part by grants from the Science Research Promotion Fund of the Japan Private School Promotion Foundation.

Funding This work was supported in part by grants from the Science Research Promotion Fund of the Japan Private School Promotion Foundation.

Compliance with ethical standards

Conflicts of interest The authors declare that there are no conflicts of interest.

Ethical approval All applicable international, national, and/or institutional guidelines for the care and use of animals were followed.

References

1. Stedman CA, Barclay ML. Review article: comparison of the pharmacokinetics, acid suppression and efficacy of proton pump inhibitors. *Aliment Pharmacol Ther*. 2000;14:963–978.
2. Bown RL. An overview of the pharmacology, efficacy, safety and cost-effectiveness of lansoprazole. *Int J Clin Pract*. 2002;56:132–139.
3. Satoh H. Discovery of lansoprazole and its unique pharmacological properties independent from anti-secretory activity. *Curr Pharm Des*. 2013;19:67–75.
4. Takagi T, Naito Y, Okada H, et al. Lansoprazole, a proton pump inhibitor, mediates anti-inflammatory effect in gastric mucosal cells through the induction of heme oxygenase-1 via activation of NF-E2-related factor 2 and oxidation of kelch-like ECH-associating protein 1. *J Pharmacol Exp Ther*. 2009;331:255–264.
5. Yoda Y, Amagase K, Kato S, et al. Prevention by lansoprazole, a proton pump inhibitor, of indomethacin -induced small intestinal ulceration in rats through induction of heme oxygenase-1. *J Physiol Pharmacol*. 2010;61:287–294.
6. Wakabayashi N, Dinkova-Kostova AT, Holtzclaw WD, et al. Protection against electrophile and oxidant stress by induction of the phase 2 response: fate of cysteines of the Keap1 sensor modified by inducers. *Proc Natl Acad Sci USA*. 2004;101:2040–2045.
7. Eggler AL, Gay KA, Mesecar AD. Molecular mechanisms of natural products in chemoprevention: induction of cytoprotective enzymes by Nrf2. *Mol Nutr Food Res*. 2008;52:S84–S94.
8. Numazawa S, Ishikawa M, Yoshida A, Tanaka S, Yoshida T. Atypical protein kinase C mediates activation of NF-E2-related factor 2 in response to oxidative stress. *Am J Physiol Cell Physiol*. 2003;285:C334–C342.
9. Keum YS. Regulation of the Keap1/Nrf2 system by chemopreventive sulforaphane: implications of posttranslational modifications. *Ann NY Acad Sci*. 2011;1229:184–189.
10. Shay KP, Moreau RF, Smith EJ, Smith AR, Hagen TM. Alpha-lipoic acid as a dietary supplement: molecular mechanisms and therapeutic potential. *Biochim Biophys Acta*. 2009;1790:1149–1160.
11. Hayes JD, McMahon M. Molecular basis for the contribution of the antioxidant responsive element to cancer chemoprevention. *Cancer Lett*. 2001;174:103–113.
12. Kawai H, Kudo N, Kawashima Y, Mitsumoto A. Efficacy of urine bile acid as a non-invasive indicator of liver damage in rats. *J Toxicol Sci*. 2009;34:27–38.
13. Ueda K, Ueyama T, Oka M, Ito T, Tsuruo Y, Ichinose M. Polaprezinc (Zinc L-carnosine) is a potent inducer of anti-oxidative stress enzyme, heme oxygenase (HO)-1—a new mechanism of gastric mucosal protection. *J Pharmacol Sci*. 2009;110:285–294.
14. Yamamoto Y, Tanahashi T, Kawai T, et al. Changes in behavior and gene expression induced by caloric restriction in C57BL/6 mice. *Physiol Genomics*. 2009;39:227–235.
15. Ueyama T, Yamamoto Y, Ueda K, et al. Is gastrectomy-induced high turnover of bone with hyperosteoidosis and increase of mineralization a typical osteomalacia? *PLoS One*. 2013;8:e65685.
16. Tanigawa T, Watanabe T, Higuchi K, et al. Lansoprazole, a proton pump inhibitor, suppresses production of tumor necrosis factor-alpha and interleukin-1beta induced by lipopolysaccharide and helicobacter pylori bacterial components in human monocytic cells via inhibition of activation of nuclear factor-kappaB and extracellular signal-regulated kinase. *J Clin Biochem Nutr*. 2009;45:86–92.
17. Yamashita Y, Ueyama T, Nishi T, et al. Nrf2-inducing anti-oxidation stress response in the rat liver–new beneficial effect of lansoprazole. *PLoS One*. 2014;9:e97419.
18. Colasanti M, Suzuki H. The dual personality of NO. *Trends Pharmacol Sci*. 2000;21:249–252.
19. Iwakiri Y, Kim MY. Nitric oxide in liver diseases. *Trends Pharmacol Sci*. 2015;36:524–536.
20. Tsuchiya H, Kaibori M, Yanagida H, et al. Pirfenidone prevents endotoxin-induced liver injury after partial hepatectomy in rats. *J Hepatol*. 2004;40:94–101.
21. Tsuji K, Kwon AH, Yoshida H, et al. Free radical scavenger (edaravone) prevents endotoxin-induced liver injury after partial hepatectomy in rats. *J Hepatol*. 2005;42:94–101.
22. Tanaka H, Uchida Y, Kaibori M, et al. Na+/H+ exchanger inhibitor, FR183998, has protective effect in lethal acute liver failure and prevents iNOS induction in rats. *J Hepatol*. 2008;48:289–299.
23. Ishizaki M, Kaibori M, Uchida Y, Hijikawa T, Tanaka H, et al. Protective effect of FR183998, a Na+/H+ exchanger inhibitor, and its inhibition of iNOS induction in hepatic ischemia-reperfusion injury in rats. *Shock*. 2008;30:311–317.
24. Nakanishi H, Kaibori M, Teshima S, et al. Pirfenidone inhibits the induction of iNOS stimulated by interleukin-1beta at a step of NF-kappaB DNA binding in hepatocytes. *J Hepatol*. 2004;41:730–736.
25. Yoshida H, Kwon AH, Kaibori M, et al. Edaravone prevents iNOS expression by inhibiting its promoter transactivation and mRNA stability in cytokine-stimulated hepatocytes. *Nitric Oxide*. 2008;18:105–112.
26. Kitade H, Sakitani K, Inoue K, et al. Interleukin 1 beta markedly stimulates nitric oxide formation in the absence of other cytokines

or lipopolysaccharide in primary cultured rat hepatocytes but not in Kupffer cells. *Hepatology*. 1996;23:797–802.
27. Sakitani K, Kitade H, Inoue K, et al. The anti-inflammatory drug sodium salicylate inhibits nitric oxide formation induced by interleukin-1beta at a translational step, but not at a transcriptional step, in hepatocytes. *Hepatology*. 1997;25:416–420.
28. Kaibori M, Okumura T, Sato K, Nishizawa M, Kon M. Inducible nitric oxide synthase expression in liver injury: liver protective effects on primary rat hepatocytes. *Inflamm Allergy Drug Targets*. 2015;14:77–83.
29. Kilkenny C, Browne WJ, Cuthill IC, Emerson M, Altman DG. Improving bioscience research reporting: the ARRIVE guidelines for reporting animal research. *PLoS Biol*. 2010;8:e1000412.
30. Smith AJ, Clutton RE, Lilley E, Hansen KEA, Brattelid T. PREPARE: guidelines for planning animal research and testing. *Lab Anim*. 2018;52:135–141.
31. Seglen PO. Preparation of isolated rat liver cells. *Methods Cell Biol*. 1976;13:29–83.
32. Kanemaki T, Kitade H, Hiramatsu Y, Kamiyama Y, Okumura T. Stimulation of glycogen degradation by prostaglandin E2 in primary cultured rat hepatocytes. *Prostaglandins*. 1993;45:459–474.
33. Horiuti Y, Ogishima M, Yano K, Shibuya Y. Quantification of cell nuclei isolated from hepatocytes by cell lysis with nonionic detergent in citric acid. *Cell Struct Funct*. 1991;16:203–207.
34. Inoue T, Horiai H, Aoki C, et al. Insulin-like growth factor-I prevents lethal acute liver failure induced by D-galactosamine and lipopolysaccharide in rats. *In Vivo*. 2003;17:293–299.
35. Guidelines for endpoints in animal study proposals. Office of Animal Care and Use, NIH http://oacu.od.nih.gov/ARAC/Endpoints.pdf. Accessed November 2017.
36. Kanzler S, Rix A, Czigany Z, et al. Recommendation for severity assessment following liver resection and liver transplantation in rats: part I. *Lab Anim*. 2016;50:459–467.
37. Green LC, Wagner DA, Glogowski J, Skipper PL, Wishnok JS, Tannenbaum SR. Analysis of nitrate, nitrite, and [15N]nitrate in biological fluids. *Anal Biochem*. 1982;126:131–138.
38. Chomczynski P, Sacchi N. Single-step method of RNA isolation by acid guanidinium thiocyanate-phenol-chloroform extraction. *Anal Biochem*. 1987;162:156–159.
39. Nishizawa M, Nakajima T, Yasuda K, et al. Close kinship of human 20alpha-hydroxysteroid dehydrogenase gene with three aldo-keto reductase genes. *Genes Cells*. 2000;5:111–125.
40. Oda M, Sakitani K, Kaibori M, Inoue T, Kamiyama Y, Okumura T. Vicinal dithiol-binding agent, phenylarsine oxide, inhibits inducible nitric-oxide synthase gene expression at a step of nuclear factor-kappa B DNA binding in hepatocytes. *J Biol Chem*. 2000;275:4369–4373.
41. Bradford MM. A rapid and sensitive method for the quantitation of microgram quantities of protein utilizing the principle of protein-dye binding. *Anal Biochem*. 1976;72:248–254.
42. Matsui K, Kawaguchi Y, Ozaki T, et al. Effect of active hexose correlated compound on the production of nitric oxide in hepatocytes. *J Parenter Enter Nutr*. 2007;31:373–380.
43. Yoshigai E, Hara T, Inaba H, et al. Interleukin-1β induces tumor necrosis factor-α secretion from rat hepatocytes. *Hepatol Res*. 2014;44:571–583.
44. Kaibori M, Yanagida H, Nakanishi H, et al. Hepatocyte growth factor stimulates the induction of cytokine-induced neutrophil chemoattractant through the activation of NF-kappaB in rat hepatocytes. *J Surg Res*. 2006;130:88–93.
45. Kleinert H, Pautz A, Linker K, Schwarz PM. Regulation of the expression of inducible nitric oxide synthase. *Eur J Pharmacol*. 2004;500:255–266.
46. Teshima S, Nakanishi H, Nishizawa M, et al. Up-regulation of IL-1 receptor through PI3 K/Akt is essential for the induction of iNOS gene expression in hepatocytes. *J Hepatol*. 2004;40:616–623.
47. Morikawa A, Sugiyama T, Kato Y, et al. Apoptotic cell death in the response of D-galactosamine-sensitized mice to lipopolysaccharide as an experimental endotoxic shock model. *Infect Immun*. 1996;64:734–738.
48. Szabó C, Módis K. Pathophysiological roles of peroxynitrite in circulatory shock. *Shock*. 2010;34:4–14.
49. Nakamura M, Matsui H, Serizawa H, Tsuchimoto K. Lansoprazole novel effector sites revealed by autoradiography: relation to helicobacter pylori, colon, esophagus and others. *J Clin Biochem Nutr*. 2007;41:154–159.
50. Sakamoto S, Okanoue T, Itoh Y, et al. Involvement of Kupffer cells in the interaction between neutrophils and sinusoidal endothelial cells in rats. *Shock*. 2002;18:152–157.
51. Bellezzo JM, Britton RS, Bacon BR, Fox ES. LPS-mediated NF-kappa beta activation in rat Kupffer cells can be induced independently of CD14. *Am J Physiol*. 1996;270:G956–G961.
52. Siebenlist U, Franzoso G, Brown K. Structure, regulation and function of NF-kappa B. *Annu Rev Cell Biol*. 1994;10:405–455.
53. Su GL. Lipopolysaccharides in liver injury: molecular mechanisms of Kupffer cell activation. *Am J Physiol Gastrointest Liver Physiol*. 2002;283:G256–G265.
54. Blackwell TS, Holden EP, Blackwell TR, DeLarco JE, Christman JW. Cytokine-induced neutrophil chemoattractant mediates neutrophilic alveolitis in rats: association with nuclear factor kappa B activation. *Am J Respir Cell Mol Biol*. 1994;11:464–472.
55. Inatomi N, Murakami I, Asano S, et al. Effect of lansoprazole and rabeprazole (E-3810) on gastric acid secretion and experimental ulcers in rats. *Jpn Pharmacol Ther*. 1997;25:2445–2454.
56. Llorente C, Jepsen P, Inamine T, et al. Gastric acid suppression promotes alcoholic liver disease by inducing overgrowth of intestinal Enterococcus. *Nat Commun*. 2017;8:837–851.